

# MULTIAXIAL LOADINGS WITH DIFFERENT FREQUENCIES BETWEEN AXIAL AND TORSIONAL COMPONENTS IN 42CrMo4 STEEL

L. Reis, G. Perpétuo, B. Li and M. de Freitas

Dept. of Mech. Engineering  
Instituto Superior Técnico  
Av. Rovisco Pais, 1,  
1049-001, Lisboa, Portugal  
E-mail:  
[luís.g.reis@ist.utl.pt](mailto:luís.g.reis@ist.utl.pt)  
[bli@ist.utl.pt](mailto:bli@ist.utl.pt)  
[mfreitas@dem.ist.utl.pt](mailto:mfreitas@dem.ist.utl.pt)

## ABSTRACT

Multiaxial loading conditions are a key issue in several mechanical components, specially when considering the effects of different frequency between the axial and the torsional stress components. This paper presents a study about the behavior of 42CrMo4 steel when subjected to multiaxial loads where the frequency of the axial solicitation is different from the torsional one. The theoretical predictions by five Critical Plane models are compared with experimental results. In addition a fractographic analysis of the fracture surfaces is carried out, as well as an analysis to the number of cycles and their intensity in each loading path.

**KEY WORDS:** Multiaxial fatigue, Non-proportional loading, Fractographic Analysis, Fatigue life prediction, Asynchronous loadings, loading paths.

## 1. INTRODUCTION

In mechanical design, studying the life of components subject to cyclic stresses, and consequently, subject to fatigue, is of utmost importance to avoid the unexpected failure of equipment, vehicles or structures. In the literature, a limited number of multiaxial fatigue experiments have been reported for tests where the applied stresses vary with different frequencies. Tests considering this factor have been performed by Mielke and Kaniut; the results are reported in Liu and Zenner [1]. Mielke and Kaniut used stress systems of two normal stresses or of one shear and one normal stress.

Similar tests have been conducted by Heidenreich [2]. Tests with two normal stresses with different frequencies have been performed by McDiarmid [3, 4], whereas Froustey [5] performed a limited number of bending and torsion tests. Both the effect of the stress waveform and the effect of different frequencies have been addressed by the tests with two normal stresses by Dietmann [6]. More recently, Bernasconi made tension-torsion tests in 39NiCrMo3 steel, [7]. However, these tests only focused on the cyclic yield strength with the variation of the frequencies between the normal and shear stress. Additionally, the author concludes that integral based models, Liu and Zenner-Papadopoulos

provided better correlation than the critical plane models, Dang Van and Findley.

Thus, the main objective of this study is to deepen knowledge on the fatigue life of the 42CrMo4 steel, especially when subjected to cyclic loading with different frequencies between axial and shear loading conditions. This material is particularly suitable for medium section components that subjected to strong solicitations due to alternate bending and torsion. The main industrial applications are in the automobile industry where it is used in gears, shafts, spindles, uprights, connecting rods and other mechanical components of high resistance. It is also used in the manufacture of moulds for plastics, [8, 9]. Given the characteristics mentioned and its application in general industry, this steel was chosen because it is representative of a material regularly used in applications where the risk of failure is highly prevalent and where it will be most valuable to obtain a deeper understanding of its fatigue behaviour.

## 2. EXPERIMENTS

The material used for the fatigue experiments is a steel of grade 42CrMo4, supplied in quenched and tempered bars of 25 mm diameter.

In Table 1 it is presented the monotonic and cyclic mechanical properties. These properties were determined by Reis [10] on previous studies.

*Table 1 - Monotonic and cyclic properties of the 42CrMo4 steel used in the experiments.*

Tensile Strength	Rm (MPa)	1100
Yield Strength	Rp (MPa)	980
Young's Modulus	E (GPa)	206
Elongation at failure	A (%)	16
Hardness	HV	362
Cyclic Yield Strength	Rp' (MPa)	540
Cyclic strength coefficient	K' (MPa)	1420
Cyclic strength exponent	n'	0.12
Fatigue strength coefficient	$\sigma_f'$ (MPa)	1154
Fatigue strength exponent	b	-0.061
Fatigue ductility coefficient	$\epsilon_f'$	0.18
Fatigue ductility exponent	c	-0.53

Specimens used in the tests were made from 25mm rod acquired through a certified company which guarantees the chemical composition of the steel and that the level of metallurgical imperfections is minimized.

Throughout the process of machining, grinding and finishing, care was taken by choosing appropriate speeds and advances in cutting tool so as not to introduce a significant increase in residual stresses and changes in surface microstructure.

After machining all specimens were polished manually with sandpaper of decreasing grain size of No. 200 to No. 1200 with the help of a small lathe. To remove marks made by the radial polishing a final sanding with 1200 grit sandpaper was then carried out in the longitudinal direction of the sample, as indicated by ASTM E 466 (2007) [11].

Figure 1 shows the dimensions and geometry of the specimens, used in the multiaxial fatigue tests, by the ASTM E606 (2004) standard.

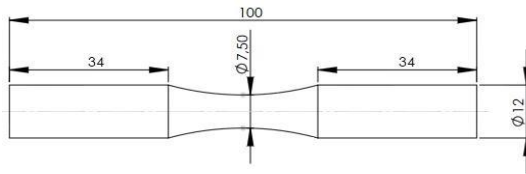


*Figure 1 - Specimen shape and dimensions in mm.*

All the tests were performed in load control mode by an Instron multiaxial tension/torsion servo-hydraulic testing system, model 8874, with a capacity of 25kN axial force and of 250N.m torque. Tests were interrupted at specimen failure or after  $1.5 \times 10^6$  cycles. In Figure 2 it is shown the experimental setup.



*Figure 2 – Experimental setup.*

In order to perform the experimental study of the influence of different frequencies between the normal and shear stress in 42CrMo4 steel, for comparison with theoretical predictions different loading paths have been defined, which are illustrated in Figure 3.

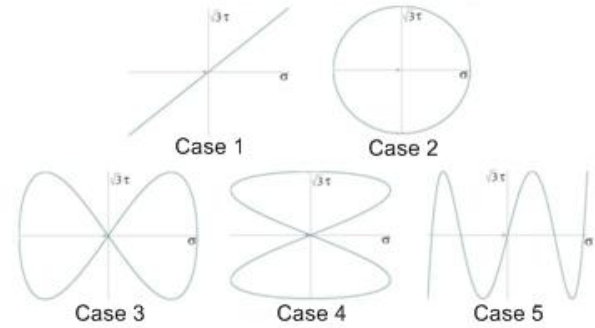


*Figure 3 - Loading paths carried out.*

Case 1 is a combination of sinusoidal loadings at the same frequency and in phase. Case 2 differs from the previous because there is a lag of  $90^\circ$  between axial and shear loading. Cases 3 and 4 result from the combination of loadings with a dual-frequency from each other and in phase start. Finally, case 5 is obtained with a torcional frequency five times higher than tension frequency and in phase start. The stress system employed is defined by  $\sigma(t) = \sigma_a \sin(\omega t) + \sigma_{mean}$  and  $\tau(t) = \tau_a \sin(\lambda \omega t) + \tau_{mean}$ . The multiaxial fatigue tests were performed with a constant stress amplitude ratio of  $\sigma = \sqrt{3}\tau$ .

### 3. THEORETICAL ANALYSIS

#### 3.1. von Mises approach

For x-y-z Cartesian system the *von Mises* equivalent stress can be written as equation (1):

$$\sigma_{eq} = \frac{1}{\sqrt{2}} \sqrt{(\sigma_x - \sigma_y)^2 + (\sigma_y - \sigma_z)^2 + (\sigma_x - \sigma_z)^2 + 6(\tau_{xy}^2 + \tau_{yz}^2 + \tau_{xz}^2)} \quad (1)$$

For biaxial loading of tension-compression with cyclic torsion the expression can be simplified, equation (2):

$$\sigma_{eq} = \sqrt{\sigma_x^2 + 3(\tau_{xy})^2} \quad (2)$$

### 3.2. Critical Plane models

Several critical plane models were considered in this study, as follows:

#### Findley criterion

Findley [12] proposed a critical plane model, which predicts that the fatigue crack plane is the plane orientation  $\theta$  with maximum Findley damage parameter, equation (3):

$$\max_{\theta} (\sigma_a + k\sigma_{a,\max}) \quad (3)$$

where  $\tau_a$  is the shear stress amplitude on a plane  $\theta$ ,  $\sigma_{n,\max}$  is the maximum normal stress on that plane  $\theta$  and  $k$  is a material parameter ( $k_{AISI303} = 0.2$ ).

#### Brown-Miller criterion

Brown and Miller [13] proposed that the shear and normal strain on the plane of maximum shear must be considered. The simplified formulation of the theory for case A cracks is (equation (4)):

$$\max_{\theta} \left( \frac{\Delta\gamma_{\max}}{2} + S\Delta\epsilon_n \right) \quad (4)$$

Critical plane is the plane of maximum shear strain range  $\Delta\gamma_{\max}$  with major value of normal strain range  $\Delta\epsilon_n$ ;  $S$  is the normal strain effects coefficient and is determined experimentally ( $S_{AISI303} = 0.2$ ).

#### Fatemi-Socie criterion

Fatemi-Socie [14] proposed a model that predicts the critical plane is the plane orientation  $\theta$  with the maximum F-S damage parameter, equation (5):

$$\max_{\theta} \left[ \frac{\Delta\gamma_{\max}}{2} \left( 1 + k \frac{\sigma_{n,\max}}{\sigma_y} \right) \right] \quad (5)$$

where  $\frac{\Delta\gamma_{\max}}{2}$  is the maximum shear strain amplitude on a plane  $\theta$ ,  $\sigma_{n,\max}$  is the maximum normal stress on that plane,  $\sigma_y$  is the material monotonic yield strength and  $k$  is a material constant ( $k_{AISI303} = 0.2$ ).

#### S-W-T criterion

Smith, Watson and Topper [15] proposed a model that predicts that the fatigue crack plane is the plane orientation  $\theta$  with maximum normal stress (the maximum principal stress), equation (6):

$$\max_{\theta} \left( \sigma_n \frac{\Delta\epsilon_1}{2} \right) \quad (6)$$

where  $\sigma_n$  is the normal stress on a plane  $\theta$ ,  $\Delta\epsilon_1$  is the principal strain range on that plane.

#### Liu criterion

Liu [16] proposed an energy method to estimate the fatigue life, based on virtual strain energy (VSE). This model considers two parameters associated with two different Modes of fatigue cracks, a tensile failure mode (Mode I),  $\Delta W_I$ , and a shear failure mode (Mode II),  $\Delta W_{II}$ . Failure is expected to occur on the plane  $\theta$  in the material, having the maximum VSE quantity. According to Mode I fracture, the parameter,  $\Delta W_I$  is, equations (7) and (8):

$$\Delta W_I = \max_{\theta} (\Delta\sigma_n \Delta\epsilon_n) + (\Delta\tau \Delta\gamma) \quad (7)$$

For Mode II fracture, the parameter,  $\Delta W_{II}$  is:

$$\Delta W_{II} = (\Delta\sigma_n \Delta\epsilon_n) + \max_{\theta} (\Delta\tau \Delta\gamma) \quad (8)$$

where  $\Delta\tau$  and  $\Delta\gamma$  are the shear stress range and shear strain range, respectively,  $\Delta\sigma_n$  and  $\Delta\epsilon_n$  are the normal stress range and normal strain range, respectively.

## 4. RESULTS AND DISCUSSION

### 4.1. Fatigue Life Results

Figure 4 presents the results of the fatigue life by the von Mises criteria for the various loading paths considered.

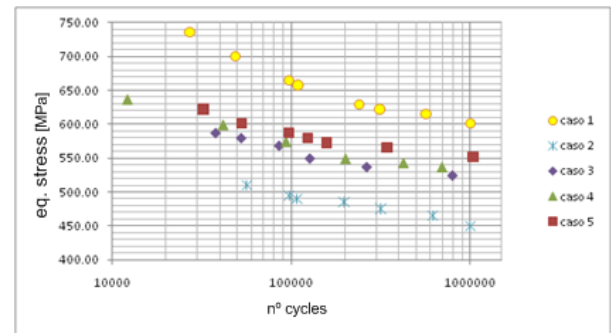
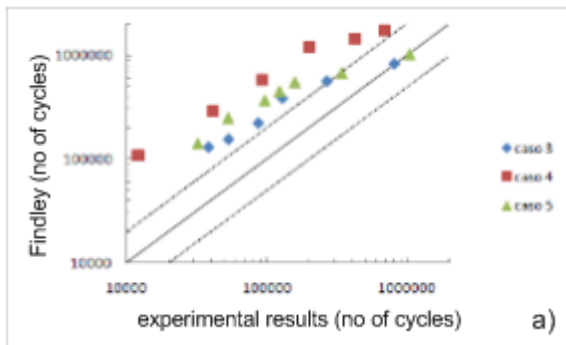


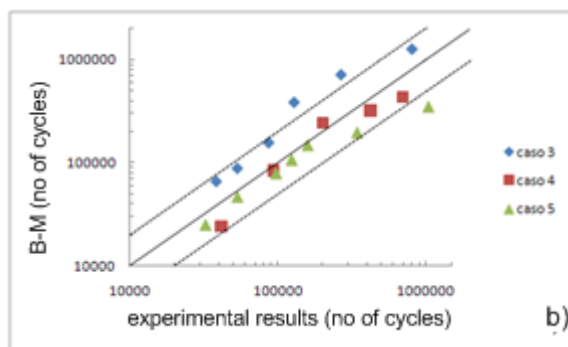
Figure 4 - Results of the fatigue life according to the von Mises criterion for steel 42CrMo4.

Since all used models, with the exception of Findley, use strain terms, it became necessary to use a cyclic plasticity model in order to predict the actual extensions after the introduction of a load control path.

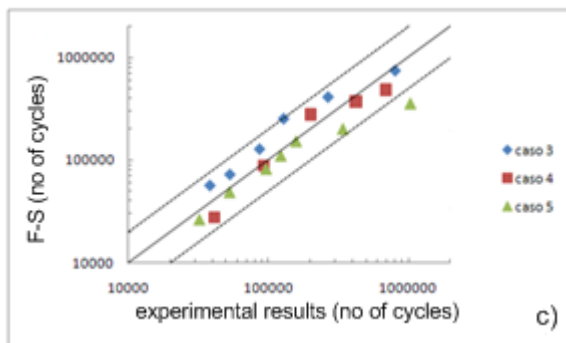
In Figure - 5 it is presented comparisons between the predictions of the models and the experimental values of fatigue life.



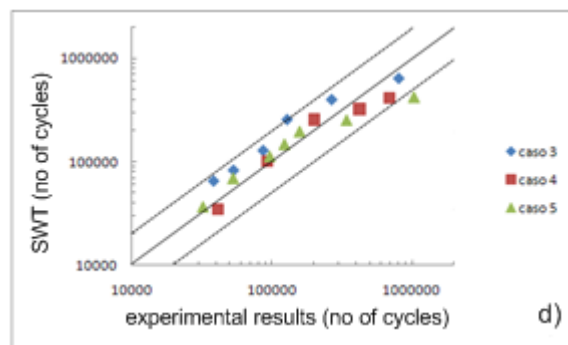
a)



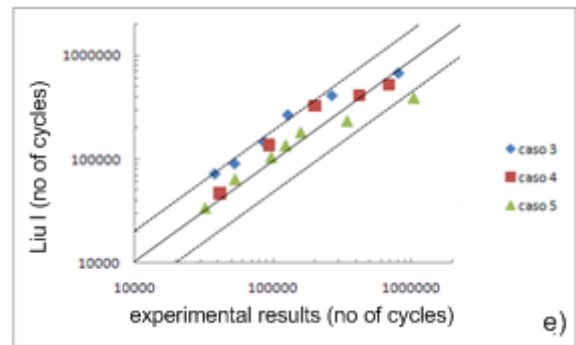
b)



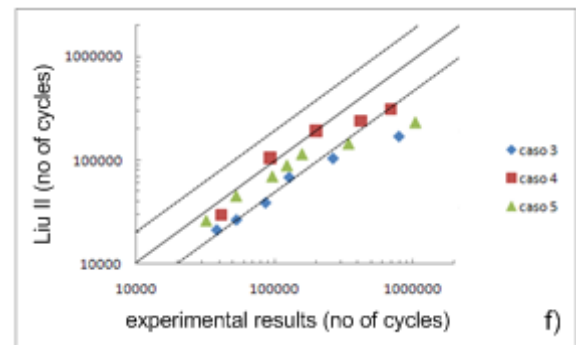
c)



d)



e)



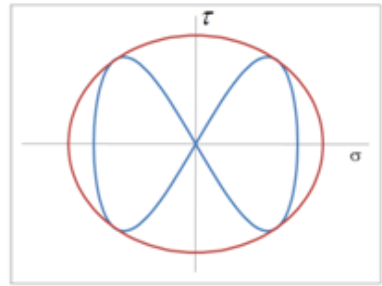
f)

Figure - 5 a) to f): Comparisons between experimental and theoretical results for the various models.

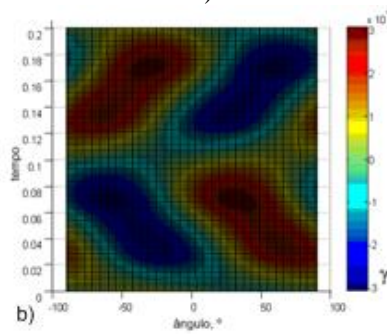
From the used models, the two which provided the worst results were the *Findley* and *Brown-Miller*, both with a greater dispersion of results and with the first presenting a too optimistic fatigue life prediction. *Fatemi-Socie*, *SWT* and *Liu I* models had the best results although being a bit optimistic predicting fatigue life for case 3. *Liu II* and *Findley* recognize that case 3 is more damaging than case 5. All remaining models reveal the same error as the models used by Bernasconi, considering that case 5 is more damaging than case 3 and 4.

Although experimental results between case 3 and 4 differ in just 2%, the used theoretical models give a larger difference in fatigue life prediction. As an example in Figure 6 it is shown the shear strain evolution over time in planes from  $-90^\circ$  to  $+90^\circ$ , for case 3.

By observing what happens in material planes, for case 3, between the two highest equivalent stresses in tension, the material is constantly being subjected to fatigue damage but in different planes. As a result, there is only one cycle of damage in each material plane. In case 4 was observed the same behaviour but in different planes, while in case 5 it was visible small sub cycles. Taking the shear strain values from the critical plane in function of time, it results the evolution depicted in Figure 7.



a)



b)

Figure 6 - a) Case 3 loading path; b) Shear strain evolution for case 3.

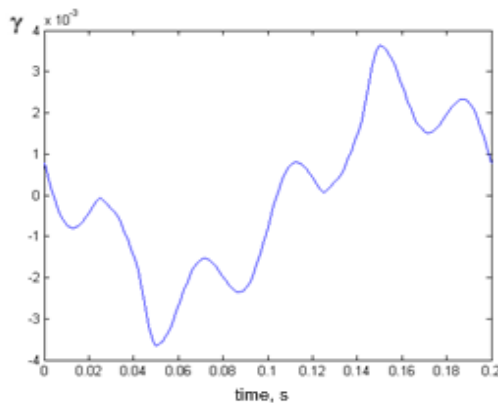


Figure 7 - Shear strain evolution in case 5.

Observing Figure 7 it is easy to identify the various existing cycles, ie, 4 sub cycles with an intensity one order of magnitude below the main cycle. As such, the expected life for the 4 sub cycles is much higher than the infinite life level being above  $10^{12}$  cycles for all methods of predicting the fatigue life, thereby, causing irrelevant material damage. It can be concluded that a good approximation to consider only a single cycle for each loading path of the cases studied in this paper.

#### 4.2. Fractographic Analysis

All fracture surfaces show a similar morphology presenting considerable crush zones in the initiation and progression of stable crack region, due to friction

caused by cyclic torsion in compression. Figure 8 shows a fracture surface of the case 5.

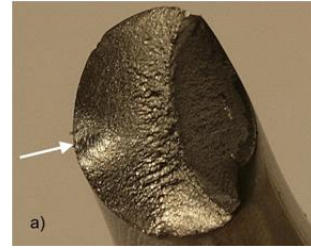


Figure 8 – Fractography of the L5.5 specimen subjected to case 5 loading path

The results obtained on the initial orientation of fatigue crack are compared with theoretical models based on the critical plane theory: *Findley*, *Brown-Miller*, *Fatemi-Socie*, *SWT (Smith, Watson and Topper)* and *Liu*. All the above models, scan each material plane  $\theta$ , from  $-90^\circ$  to  $+90^\circ$  in order to seek for the critical plane, ie, the plane for which the specific parameter of damage is maximized. Figure 9 shows an example for the SWT model. Table 2 presents a comparison between measured and predicted crack angles.

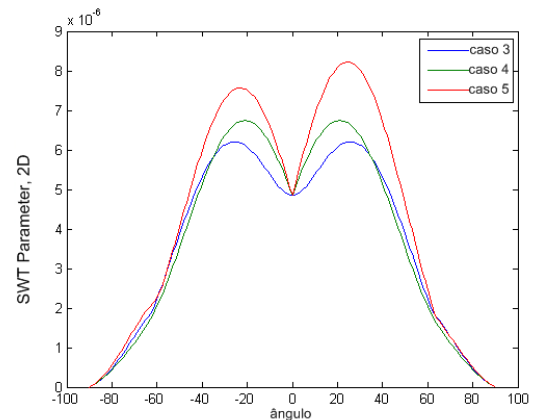


Figure 9 - Evolution of the SWT parameter on different planes for different loading paths.

Table 2 - Measured and predicted initial crack angles.

Loading Path	Case 3		Case 4		Case 5	
Specimen	L2.5	L2.6	L05.5	L05.6	L5.5	L5.6
Measured angle	+26	-18	-23	-20	-20	-22
Findley	$\pm 18$		$\pm 21$		-21/+23	
Brown Miller	$\pm 17/\pm 73$		$\pm 23/\pm 67$		-20/+70	
FS	$\pm 17/\pm 73$		$\pm 23/\pm 67$		-20/+70	
SWT	$\pm 25$		$\pm 21$		-23/+25	
Liu I	$\pm 26$		-21		-21/+25	
Liu I	$\pm 17/\pm 73$		$\pm 21/\pm 67$		-20/+70	

After analyzing the data presented in Table 2, it can be concluded that, in general, there was a good match between the theoretical models and experimental measurements from the specimens. With the exception of the specimen L2.5, all others have a maximum error of only 3° compared to theoretical models.

## 5. CONCLUSIONS

The cases taken as reference, cases 1 and 2, respectively, are the cases that minor and major damage cause to the material. Among the remaining cases, case 5 does less damage to the material and case 3 is the one that causes greater damage.

Excluding the proportional loading path, greater frequency relation between stress components causes less damage.

All critical plane criteria produced reasonable estimates of crack initiation angles by comparison with the experimental results.

Critical plane criteria based only in stress terms (*Findley*) or in strain terms (*Brown-Miller*) are less effective in predicting the fatigue life. Criteria with both stress and strain terms (*Fatemi-Socie*, *SWT* and *Liu*) are more likely to consider the features of each type of loading.

Criteria developed for materials with predominant failure mode I (*SWT* and *Liu I*) had good results for predicting the fatigue life of the 42CrMo4 steel in mentioned conditions.

For a correct fatigue life prediction, the use of a plasticity model to predict the actual strain values is essential.

For the axial-shear relation studied, sub cycles present in the various loading path do not show relevant magnitude to cause relevant damage.

## ACKNOWLEDGEMENTS

The authors gratefully acknowledge financial support from FCT - Fundação para Ciência e Tecnologia (Portuguese Foundation for Science and Technology), through the project POCTI/EME/59577/2004.

## REFERENCES

- [1] Liu J, Zenner H. Fatigue limit of ductile metals under multiaxial loading. In: Carpinteri A, de Freitas M, Spagnoli A, editors. Biaxial/ multiaxial fatigue and fracture, ESIS 31. Amsterdam: Elsevier; 2003. p. 147–63.
- [2] Heidenreich R, Richter I, Zenner H. Schubspannungsintensitätshypothese – weitere experimentelle und theoretische Untersuchungen. Konstruktion 1984;36:99–104.
- [3] McDiarmid DL. Fatigue under out-of-phase biaxial stresses of different frequencies. In: Miller KJ, Brown MW, editors. Multiaxial fatigue, ASTM STP 853. Philadelphia: ASTM; 1985. p. 606–21.
- [4] McDiarmid DL. Mean stress effects in biaxial fatigue where the stresses are out-of-phase and at different frequencies. In: Kussmaul K, McDiarmid DL, Socie D, editors. Fatigue under biaxial and multiaxial loadings, ESIS 10. London: Mechanical Engineering Publications; 1991. p. 321–35.
- [5] Froustey C. Fatigue multiaxiale en endurance de l'acier 30 NCD 16. Thèse de l'Ecole Nationale Supérieure d'Arts et Métiers, Bordeaux; 1987.
- [6] Dietmann H, Bhongbhibhat T, Schmid A. Multiaxial fatigue behaviour of steels under in-phase and out-of-phase loading, including different wave forms and frequencies. In: Kussmaul K, McDiarmid DL, Socie D, editors. Fatigue under biaxial and multiaxial loadings, ESIS 10. London: Mechanical Eng. Publications; 1991. p.449–64.
- [7] A. Bernasconi, S. Foletti, I.V. Papadopoulos, (2008) "A study on combined torsion and axial load fatigue limit tests with stresses of different frequencies". Int. Journal of Fatigue 30 (2008) 1430–1440.
- [8] Shang, D-G., Sun, G-Q., Deng, J., Yan, C-L., "Multiaxial fatigue parameter and life for a medium-carbon steel based on critical plane approach". Int. Journal of Fatigue (2007)
- [9] Reis, L., Li, B., Freitas, M., (2007). "Evaluation of a Multiaxial Fatigue Models for a Structural Steel (42CrMo4), "8° International Conference on Multiaxial Fatigue & Fracture"
- [10] Reis, L., (2004). "Comportamento Mecânico de Aços em Fadiga Multiaxial a Amplitude de Carga Constante e Síncrona", Universidade Técnica de Lisboa, IST, PhD Thesis in Portuguese.
- [11] ASTM E 466 (2007). Standard Practice for Conducting Force Controlled Constant Amplitude Axial Fatigue Tests of Metallic Materials1.
- [12] Findley, W. N. (1956). "Theory For Combined Bending And Torsion Fatigue With Data For SAE 4340 Steel", Int. Conf. Fatigue Metals: 150-157.
- [13] Brown, M., Miller, K. J. (1973). "A Theory for Fatigue Failure Under Multiaxial Stress-strain Conditions." Proceedings of the Institute of Mechanical Engineers 187: 745-755.
- [14] Fatemi, A., Socie, D. (1988). "A Critical Plane Approaches to Multiaxial Fatigue Damage including Out-of-Phase Loading", FFEMS 11(3): 149-165.
- [15] Smith, K. N., Watson, P., Topper, T. H. (1970). "A Stress-Strain Function for the Fatigue of Metals", J. of Materials, JMLSA 5(4): 767-778.
- [16] Liu, K. (1993). "A Method Based on Virtual Strain-Energy Parameters for Multiaxial Fatigue Life Prediction", Advances in Multiaxial Fatigue, ASTM STP 1191: 67-84.